Science Arts & Métiers (SAM)

is an open access repository that collects the work of Arts et Métiers Institute of Technology researchers and makes it freely available over the web where possible.

This is an author-deposited version published in: https://sam.ensam.eu
Handle ID: .http://hdl.handle.net/10985/26092

To cite this version :

Emmanuel RICHAUD, Justine DELOZANNE - Thermal oxidation of diallylbisphenol A - bismaleimide networks. Comonomer effect and kinetic modelling - Polymer Degradation and Stability - Vol. 219, p.110628 - 2024

Any correspondence concerning this service should be sent to the repository Administrator : scienceouverte@ensam.eu

Arts et Métiers Institute of Technology

THERMAL OXIDATION OF DIALLYLBISPHENOL A - BISMALEIMIDE NETWORKS. COMONOMER EFFECT AND KINETIC MODELLING

Emmanuel RICHAUD[1,*], Justine DELOZANNE[2]

1. Laboratoire PIMM, Arts et Metiers Institute of Technology, CNRS Cnam, HESAM Universite, 151 boulevard de l'Hopital, Paris 75013, France

2. SAFRAN Composites, 33 avenue de la Gare, 91760, Itteville, France

* corresponding author: emmanuel.richaud@ensam.eu

ABSTRACT

Pure BMI resin based on 4,4'-bismaleimidodiphenylmethane (BMI) and its copolymers with various quantities of 2,2'-diallylbisphenol A (BMI-DABPA 2-1, BMI-DABPA 1-1, BMI-DABPA 1-2) were thermally aged. Ageing at 160°C was monitored by FTIR and showed the greatest reactivity of diallyl groups which accelerate the degradation of BMI-DABPA copolymers. It was confirmed by a gravimetric study of ageing under nitrogen or oxygen at 350 and 375°C. A co-oxidation kinetic model was proposed for describing the oxidation of BMI and BMI-DABPA systems. The effect of the main kinetic parameters was discussed from a parametric study. The main rate constants were estimated from the fitting of experimental curves and comparable gravimetric data from literature.

KEYWORDS

Bismaleimide resins, 2,2′-Diallylbisphenol A, thermal oxidation, mass loss, kinetic modelling

1. INTRODUCTION

BMI resins were first obtained from homopolymerization of bismaleimide monomers, the most common one being the 4,4'-bismaleimidodiphenylmethane (Figure 1a). Polymerization can be achieved even in absence of peroxide or imidazole catalysts [1,2,3] and gives networks with high glass transition (300°C or more) [3,4] and interesting mechanical properties (specific strength at break) but displaying a poor toughness (below 1 MPa.m$^{1/2}$) [4,5]. Many strategies were implemented for improving

this latter such as (i) increasing the distance between crosslink nodes or (ii) adding comonomers such as for example 2,2'-diallylbisphenol A (DABPA – Figure 1b). This is the case of existing commercial systems such Matrimid 5292 [6]. For example, a Allyl + BMI « copolymer » [7] displays stress at break and impact resistance are respectively around 145 MPa and 12 $kJ.m^{-2}$, which is much higher than data given for the « homopolymer » BMI (40-80 MPa for stress at break [4] and impact strength around 8 $kJ.m^{-2}$ [8]).

Such materials are usually employed in demanding applications where thermal stability is crucial. Previous works address the case of various homopolymers where the non-reactive group between maleimide groups was changed [9,10,11]. However, there is, to the best of our knowledge, very few studies [12,13] dealing with the effect of comonomers and in particular the effect of the BMI/diallyl stoichiometric ratio on thermal stability.

Degradation of pure BMI was mostly investigated in non-isothermal conditions by means of classical TGA tests [9,10,11]. However, isothermal ageing studies exist but are scarce [9,14,15,16], which limits the understanding of the degradation mechanism.

Ageing experiments must in general be used for predicting lifetime in service conditions. For that purpose, it is well established that a kinetic model must be used. Kinetic parameters must correspond to elementary processes involved in degradation, and obey Arrhenius law. The simulation of experimental results allows an estimation of the values of the parameters used in kinetic models in accelerated conditions. The extrapolation of those values at service temperatures allows to predict the degradation rate at those conditions. A « proof of concept » of the predictive capability of kinetic model was published by Colin et al [17] who successfully simulated the mass loss kinetics of a BMI based material. However, the proposed kinetic model corresponds to the simple case where there is only one sort of reactive unit in the material, which is clearly not the case in the case of BMI-DABPA networks.

In this paper, we will hence synthesize and degrade samples with various alkyl/maleimide stoichiometry's in order to:

- investigate the effect of comonomers on stability for isothermal ageing under nitrogen, or under oxygen by performing isothermal tests,

- characterize the chemical trackers of oxidation in link with the BMI-DABPA formulation,

- discuss on the effect of DABPA and propose a first kinetic model of degradation for pure BMI and BMI-DABPA copolymers. We will focus on its capability to simulate mass loss since this latter is linked to shrinkage and latter cracking [18,19].

2. EXPERIMENTAL

2.1. Materials

Materials were synthesized using two comonomers given in Figure 1: 4,4'-Bismaleimidodiphenylmethane (CAS: 13676-54-5 - ref 227463-100G supplied by Sigma Aldrich) and 2,2′-Diallylbisphenol A (CAS: 1745-89-7 – ref 413526-100ML supplied by Sigma Aldrich).

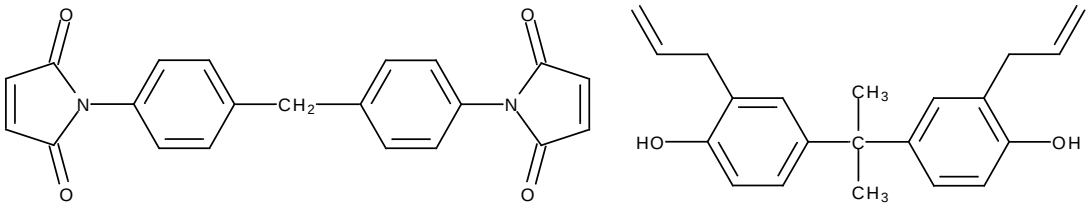

(a) (b)

Figure 1. Structure of 4,4'-Bismaleimidodiphenylmethane (a) and 2,2',diallylbisphenol A (b).

Materials were obtained from the following curing cycles:

- for BMI films: Thickening of reactive mixture during 10 min at 170°C, then 10 min at 175°C after which samples were pressed using a laboratory press (240 bars without use of spacer) during 1 h at 180°C + 1 h à 190°C + 2 h à 200°C. The obtained films have a thickness about 40 µm.

- for BMI-DABPA films: Thickening of reactive mixture during 30 min at 150°C + 20 min at 180°C after which samples were pressed using a laboratory press (240 bars without use of spacer)1 h at 180°C + 1 h at 190°C + 2 h at 200°C. The obtained films have a thickness about 20 µm. Copolymers are detailed in Table 1.

2.2. Exposure conditions

Samples were aged in ventilated ovens (AP60, SCS, France) under atmospheric air at 160°C. Ageing was monitored by FTIR and elemental analysis.

Ageing under 100% N_2 or 100% O_2 atmosphere was performed in situ in TGA cell.

2.3. Characterization methods

2.3.1. ThermoGravimetric Analysis

TGA measurements were performed using a Q500 apparatus driven by QSeries Explorer (TA Instruments). After a 20°C min^{-1} heating, isothermal degradation was performed at a constant temperature equal to 350 and 375°C either under 100% N_2 or 100% O_2 atmosphere supplied by a continuous 50 $ml.min^{-1}$ gas flow.

2.3.2. Fourier Transform InfraRed spectroscopy

FTIR spectroscopy in transmission mode was carried out using a Frontier spectrophotometer (PerkinElmer) by averaging 8 scans at 1 cm^{-1} resolution between 400 and 4000 cm^{-1}.

2.3.3. Elemental Analysis

Carbon and hydrogen measurements were performed on a homemade Carbon / Hydrogen elemental micro-analyzer (Institut des Sciences Analytiques, UMR5280 CNRS, Villeurbanne). About 1.5 mg of sample weighted in silver cups (3.2 × 6, Säntis Analytical AG, Teufen, Switzerland) dropped into a unit combustion in a flow of 50 $ml.min^{-1}$ of pure oxygen. The combustion system is equipped by two furnaces held at 1050°C for the upper one and 850°c for the lower and contain a vertical glass combustion tube, half filled with 11 cm of CuO oxidation catalyst (Copper oxide wire 0.7mm, Säntis Analytical) and silver wool (Silberwolle Carl ROTH GmbH, Karlsruhe, Germany) used as halogens trap. Carbon and hydrogen have been respectively turned into carbon dioxide (CO_2) and water (H_2O). The measurements of both molecules have been done using a CO_2/H_2O non-dispersive infrared detector (Rosemount NGA 2000). A calibration has been daily established by measuring standards references (molecules pure at 99.9%). Then up to 8 samples were injected. To be sure of the lack of calibration-drift, 2 standards reference were introduced and measured as sample, every eight analyses. The uncertainty of measurements has been determined at +/-0.10 for H measurement and +/- 0.30 for carbon measurement. Reference standards used for calibration and stability controls are high purity compounds purchased from Sigma Aldrich corp. (Saint-Louis, Missouri, USA): Methionine (C: 40.25 %, H: 7.43 %), Glycine (C: 36.36%, H: 6.10%), Taurine (C: 19.20%, H: 5.20%), Cystine (C: 29.99%, H: 5.03%), Valine (C: 51.26, H: 9.46%), Tryptophan (C: 64.69%, H: 5.92%).

3. RESULTS

3.1. Thermal stability

The thermal stability of systems was first investigated by studying in situ degradation of BMI and BMI-DABPA networks using TGA either under inert atmosphere or under pure oxygen at elevated temperatures (350 and 375°C) as shown in Figure 2. The following conclusions can be drawn:

- BMI can be considered as relatively stable under inert atmosphere (less than 1% mass loss) consistently with literature data [9] but the addition of DABPA comonomer promotes thermal degradation.

- The presence of oxygen accelerates the degradation rate.

- In presence of oxygen, the DABPA also accelerates degradation compared to pure BMI. However, differences between BMI-DABPA 2-1, BMI-DABPA 1-1 and BMI-DABPA 1-2 under oxygen are weaker than for degradations under nitrogen. BMI-DABPA 1-2 always is the less stable material for ageing under inert atmosphere, but this is not necessarily the case under oxygen. A definitive explanation would need to finely characterize the structure of copolymers with high DABPA content (presence of homopolymerized DABPA sequences) and the stabilizing effect of phenolic groups, which is out of reach using basic laboratory tools used in this work.

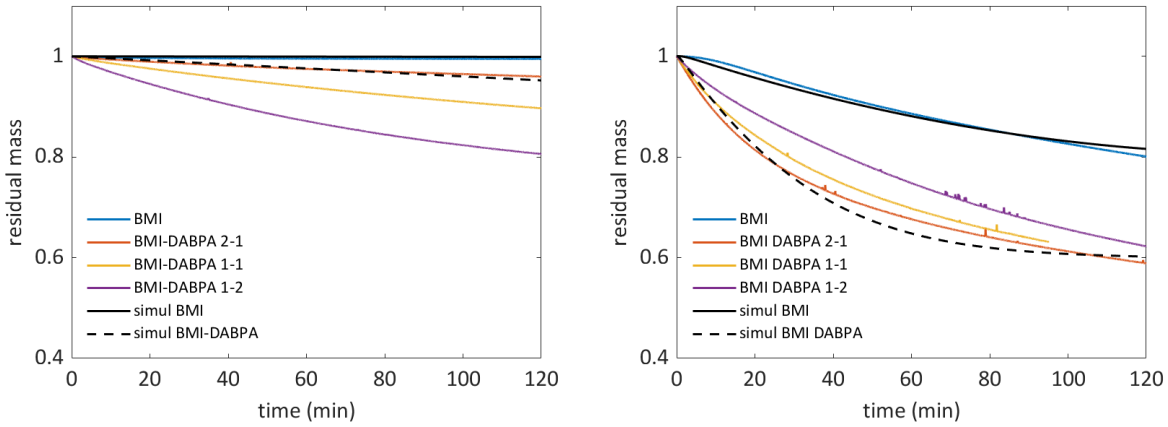

(a) (b)

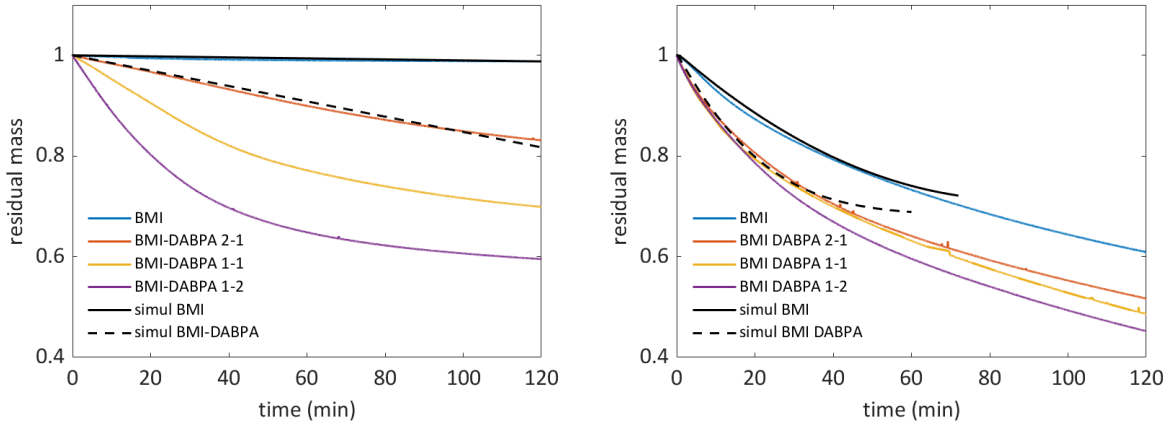

(c) (d)

Figure 2. Mass loss curves of BMI and BMI-DABPA at 350°C (a, b) and 375°C (c, d) under inert atmosphere (a, c) and oxygen (b, d). Full lines correspond to kinetic modelling described in « Discussion » section.

3.2. Chemical changes

Samples were first characterized by elemental analysis. Results are given in Table 1 and confirm an acceptable reliability of the method for characterizing the structure of unaged materials.

		BMI	BMI-DABPA 2-1	BMI-DABPA 1-1	BMI-DABPA 1-2
BMI weight ratio		1	0.699	0.538	0.368
theoretical	%C	0.704	0.738	0.757	0.776
	%O	0.179	0.156	0.144	0.131
	%H	0.039	0.051	0.057	0.064
experimental	%C	0.693	0.699	0.713	0.702
	%O	0.188	0.159	0.187	0.205

	%H	0.039	0.048	0.059	0.056

Table 1. Mass composition of the reactive mixture and elemental analysis of BMI and BMI-DABPA networks.

During thermal ageing, all materials display an increase in their oxygen content (illustrated as the ratio of oxygen concentration over carbon one [20]). Despite some outliers, data also confirm that BMI-DABPA copolymers oxidize faster than BMI homopolymer.

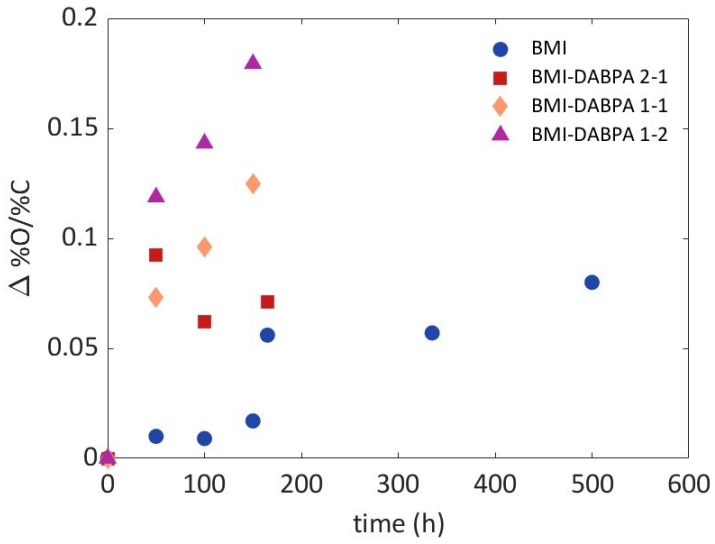

Figure 3. Changes in elemental analysis.

In order to go further in the understanding of chemical structure and its changes, FTIR spectra analysis were performed for unaged and aged samples. Spectra for unaged samples in several regions are given in Figure 4.

As expected from their theoretical structure given in Scheme 1, BMI homopolymers are mainly characterized by the methylene groups at 2930 cm^{-1} (Figure 4a) and the presence of residual double bonds concentration (Figure 4d).

The main following differences due to DABPA comonomer can be observed:

- the stretching of hydroxyl bond at around 3400 cm^{-1} (Figure 4a)

- the stretching of C-H in methyl groups CH_3 at 2970 cm^{-1} (Figure 4b)

- the C-O stretching of phenol groups at 1250 cm^{-1} (Figure 4c)

- the out of plane bending of alkenes in the 600 – 1000 cm^{-1} (Figure 4d). Here, absorbances of allyl at 989 and 914 cm^{-1} [13] are not detected, meanwhile 832 ($\delta_{C=C}$ in BMI) and 690 cm^{-1} ($\delta_{C=C-H\ cis}$ in BMI) absorbances still seem present. It would suggest that networks are not fully polymerized [1]. We however did not try to optimize curing degree, keeping in mind that post-curing must occur in situ during the heating ramp prior to 350 and 375°C isothermal ageing for the experiments reported in Figure 2.

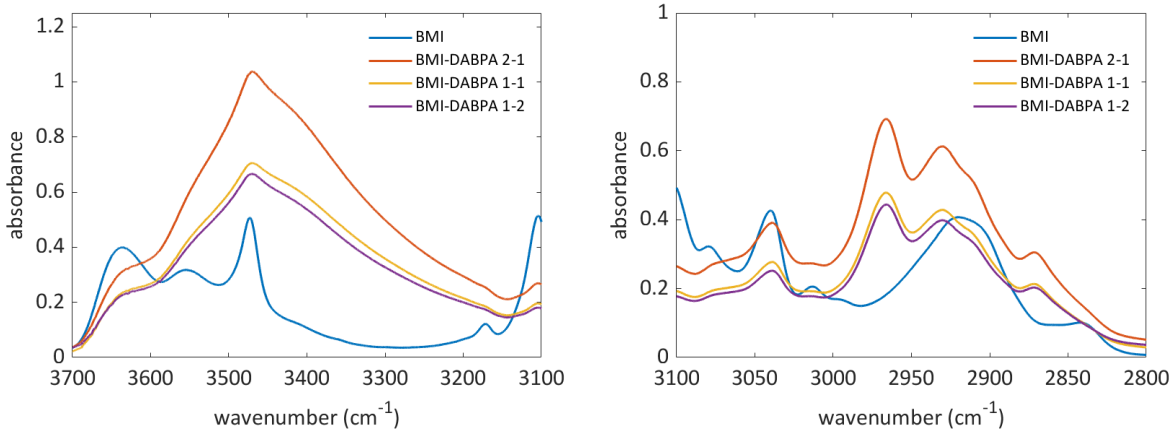

(a) (b)

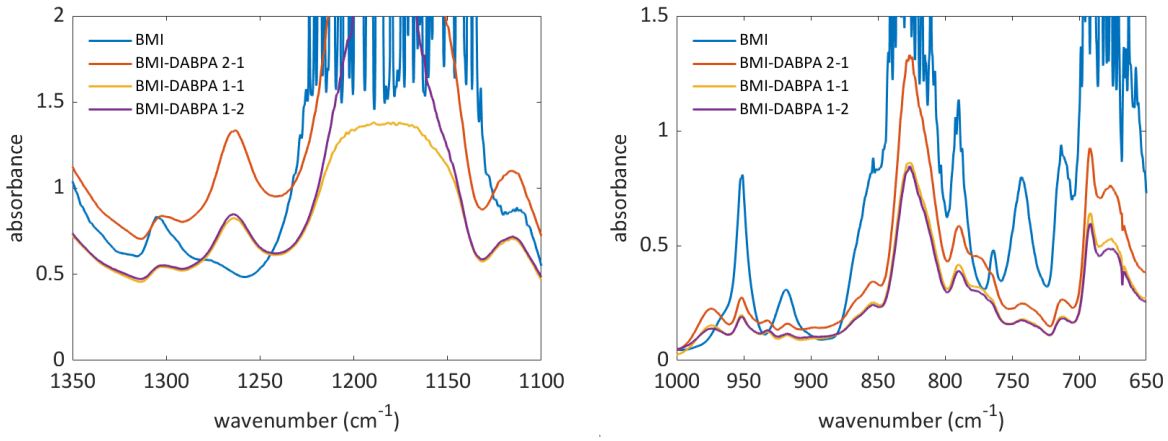

(c) (d)

Figure 4. InfraRed spectra of BMI homopolymer and BMI-DABPA copolymers in the region of hydroxyls (a), C-H stretching (b), fingerprint (c) and C=C double bond bending region (d).

After thermal ageing at 160°C, the following differences (discussed in the following of this paper) were systematically observed (Figures 5 and 6):

- an increase in the carbonyl region, more specifically in the 1600 to 1700 cm^{-1} wavenumber range, which could correspond to the appearance of benzophenone functions, or any other kinds of conjugated ketones, consistently with previous results [16,[21]].

- the disappearance of aromatic =C-H stretching (above 3000 cm^{-1}) which may be due to volatile loss (see above) or isomerization. Actually, the appearance of a new absorbance at 930 cm^{-1} accompanied by the increase of a sharp band at 1610 cm^{-1}, could correspond to the appearance of new >C=C< double bonds (see also Supplementary information SI-1).

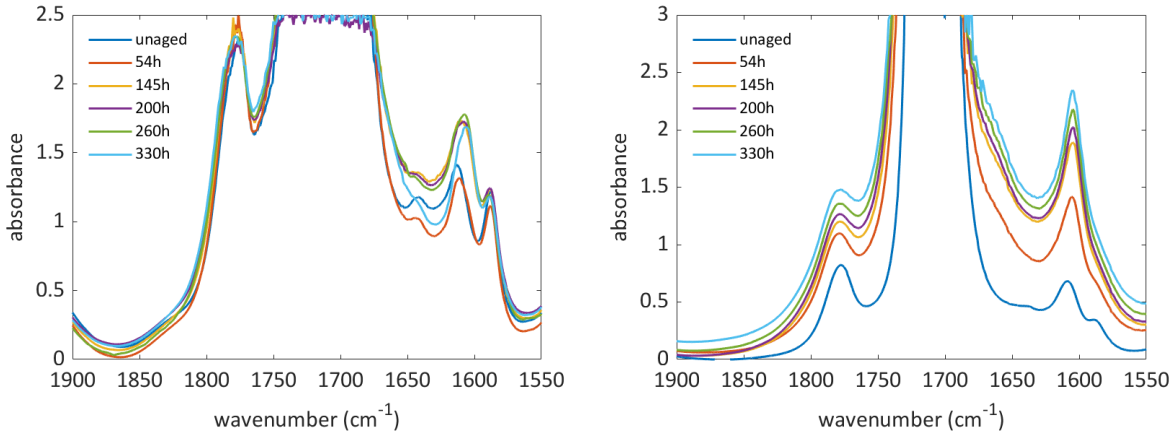

(a) (b)

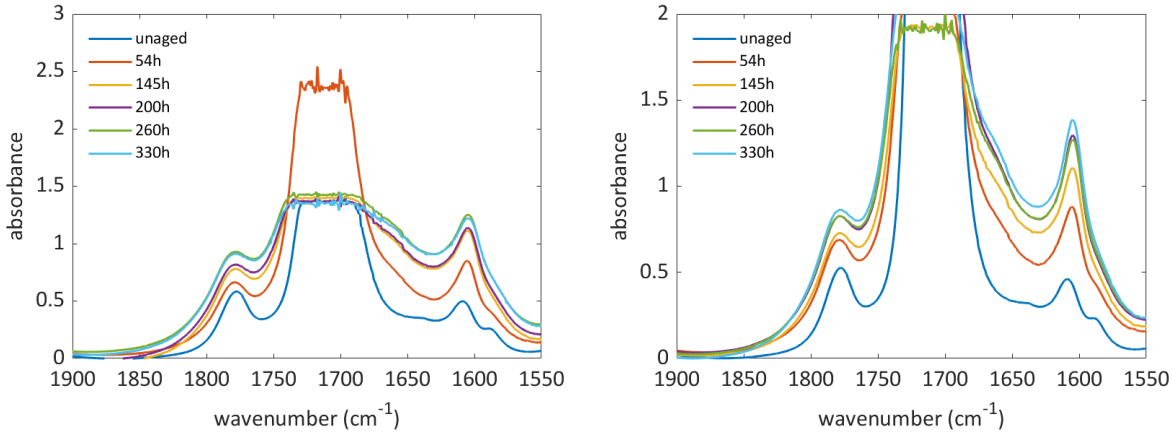

(c) (d)

Figure 5. FTIR spectra in the carbonyl region for BMI (a), BMI-DABPA 2-1 (b), BMI-DABPA 1-1 (c) and BMI-DABPA 1-2 (d) thermally oxidized at 160°C under air.

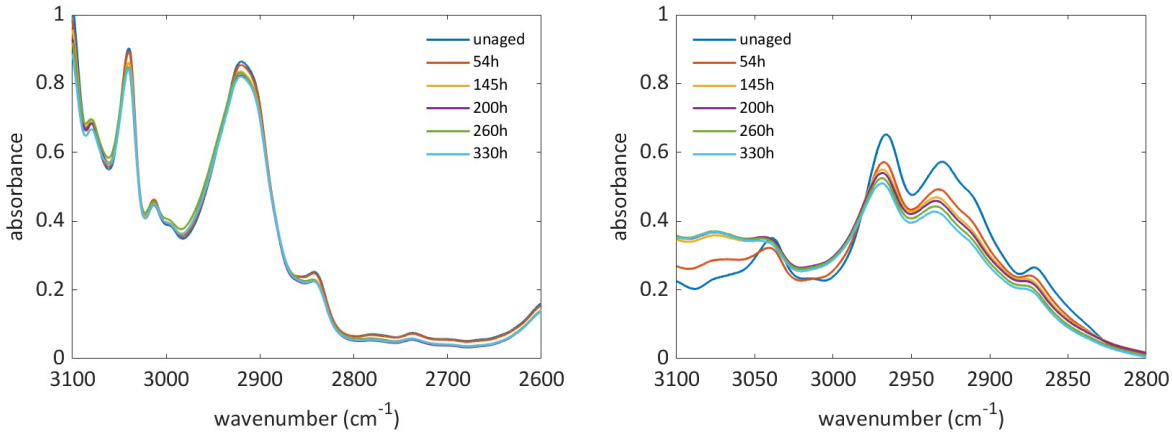

(a) (b)

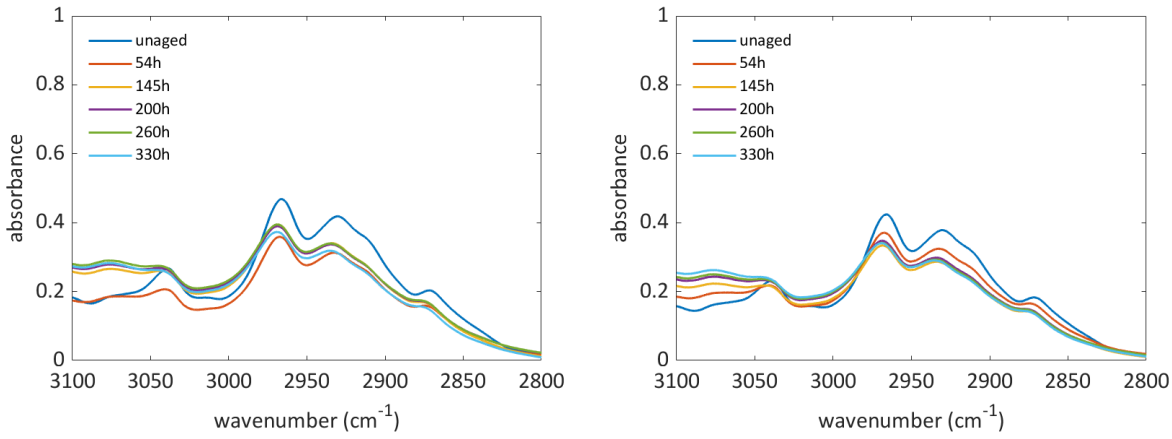

Figure 6. FTIR spectra in the C-H stretching region for BMI (a), BMI-DABPA 2-1 (b), BMI-DABPA 1-1 (c) and BMI-DABPA 1-2 (d) thermally oxidized at 160°C under air.

Finally, our results unambiguously show that the use of DABPA as comonomer is detrimental to thermal stability of BMI based resins, either under nitrogen or in presence of oxygen.

4. DISCUSSION

The first aim of this section is to propose an explanation of the chemical changes in link with the initial structure of networks, and try to explain why diallylbisphenol A lowers thermal stability of BMI-DABPA copolymers. The second aim is to propose a reasonable kinetic model based on the reactivity of each comonomer so as to describe the reactivity of the family of BMI-DABPA networks.

4.1. Structural changes observed in BMI-DABPA

Let us start by recalling the theoretical structure of BMI and BMI-DABPA 2-1 copolymers (Scheme 1). In BMI homopolymers, the polymerization occurs along the double bonds (even in absence of radical initiator), as depicted in Scheme 1. In BMI-DABPA copolymers, polymerization occurs in two stages: a Michael addition of alkene (hold by diallylbisphenol A) followed by a Diels Alder reaction with another bismaleimide group. The ideal stoichiometry is here one diallyl group for two maleimides ones.

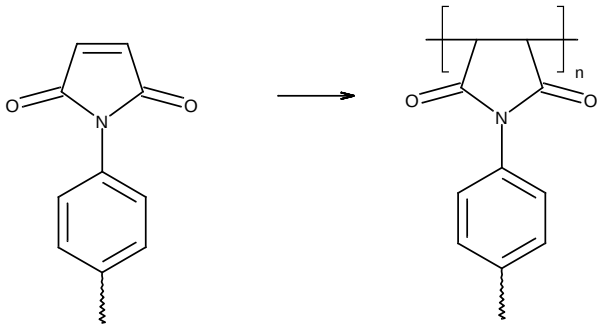

(a)

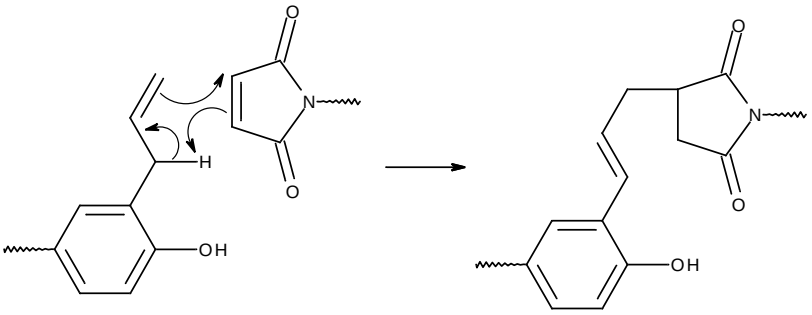

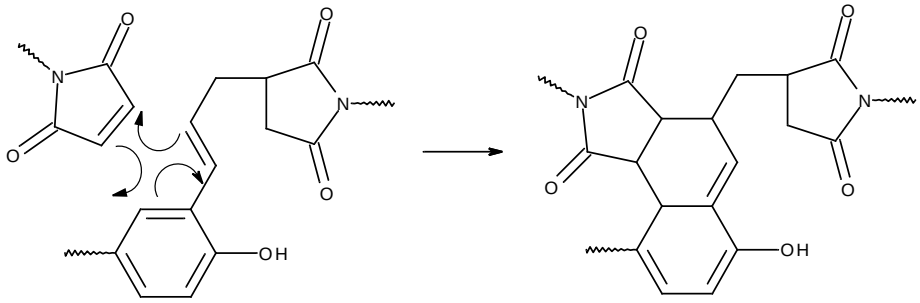

(b)

Scheme 1. Curing mechanism in BMI (a) and BMI-DABPA (b).

Since only BMI and BMI-DABPA 2-1 correspond to well defined structures, we will focus on those two networks in the following, keeping in mind that thermal stability of BMI-DABPA 2-1, BMI-DABPA-1-1 and BMI-DABPA 1-2 seem somewhat close.

To better understand the differences in terms of “structure-stability relationships”, some representative units of BMI homopolymer and BMI-DABPA 2-1 groups were analyzed using a recently

developed Machine Learning tool (Alfabet) allowing the determination of Bond Dissociation Energies, and the possible « Achylle Heel » of each kind of polymer. Such an approach was recently successfully tested on epoxies [22]. Using SMILES codes given in Supplementary Information SI-2, some BDE corresponding to weak groups are given in Figure 7.

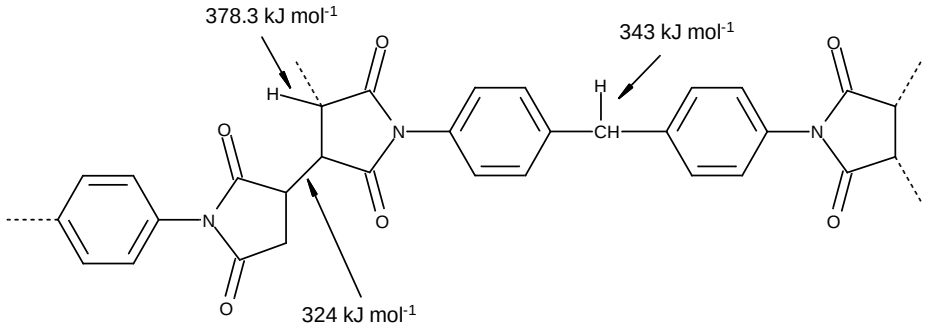

(a)

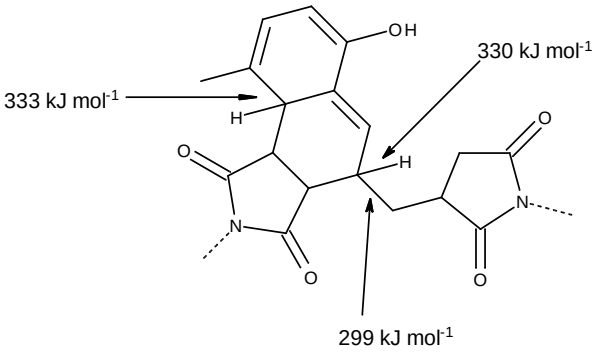

(b)

Figure 7. Machine learning based estimation of some Bond Dissociation Energies in BMI (a) and BMI-DABPA 2-1 (b).

During oxidation, the appearance of signal located at around 1650 cm^{-1} could come from the oxidation of central methylene as depicted in Scheme 2. It is also possible to envisage that diphenyl substituted methylene alkyl radicals isomerize and generate cyclohexadienone products. As proposed in Scheme 2b, it may explain why both absorbances of aliphatic and aromatic C-H seem to decrease (see Figure 6a).

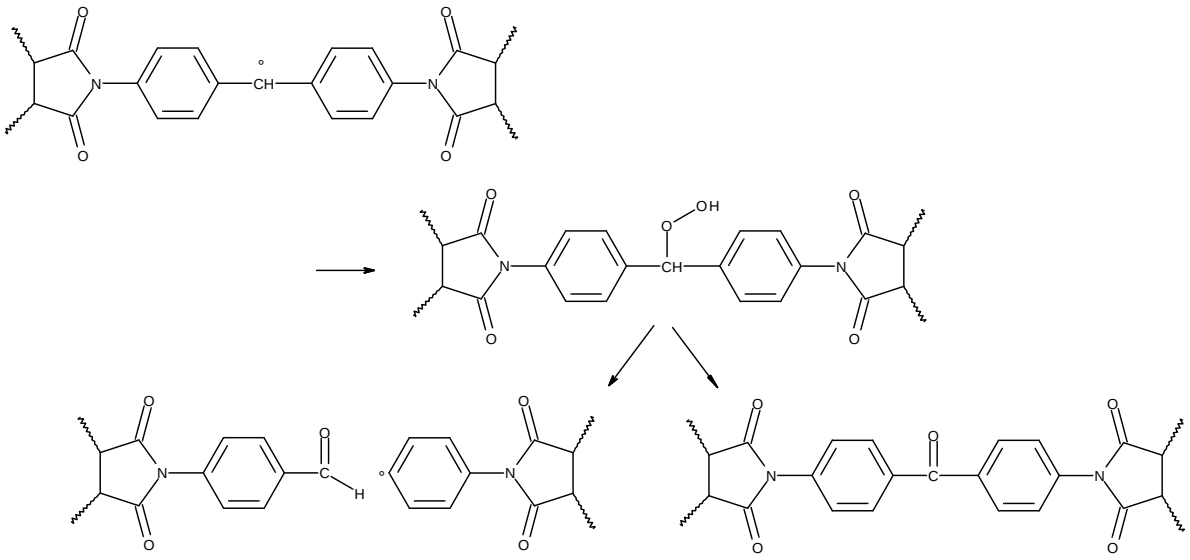

(a)

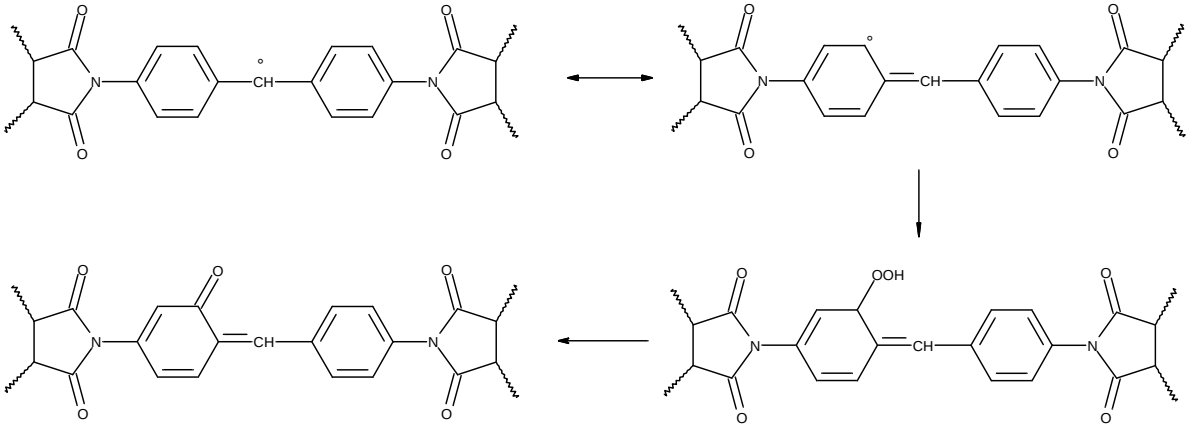

(b)

Scheme 2. Possible oxidation mechanism of BMI homopolymer) (a) or with (b).

In the case of copolymer, it seems clear that the allylic C-H are easily oxidized into various kinds of ketones. In the case of copolymers, it is hence not surprising that the carbonyl region displays a new signal located between 1750 et 1800 cm^{-1}.

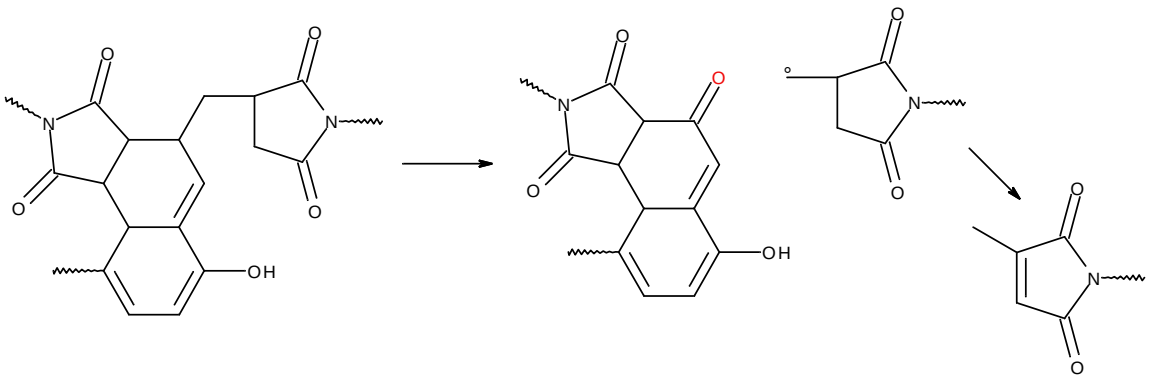

(a)

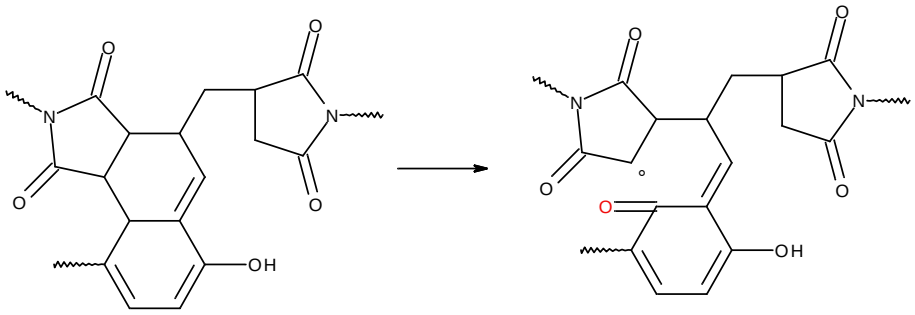

(b)

Scheme 3. Oxidation of allylic sites in BMI-DABPA.

The qualitative comparison of oxidized spectra for BMI homopolymer and BMI-DABPA copolymers suggests that copolymers are less stable than homopolymers. This is well in line with elemental analysis results. Dealing now with mass loss curves, it seems that oxidation generates more volatile compounds in the case of copolymers. We will now try to derive a kinetic model for describing the degradation kinetic and in particular mass loss curves of materials.

4.2. Kinetic modelling

We based on the general mechanistic scheme used for describing the oxidation of several polymers. This latter was in particular implemented for describing the oxidation of bismaleimide networks by Colin et al [17]. In its initial formulation, the model assumed that maleimides were the only reactive sites which is not the case here since there are strong discrepancies between BMI and BMI-DABPA 2-1. Instead of using a simple model with « genuine » constants for BMI and BMI-DABPA systems, we decided to develop a cooxidation kinetic model [23,24] where reactive sites for BMI (subscript 1) and DABPA (subscript 2) react independently or by crossed reactions and where the reactivity of BMI-

DABPA copolymers is ruled by rates constants specific to each site. Moreover, our results (in particular of mass loss data under inert atmosphere) showed the existence of a « pure » thermolytical process that we simply modeled by reaction (0) generating two alkyl radicals and (4) corresponding to their termination by coupling. The mechanistic scheme is written as follows:

Initiation	$P_1H \rightarrow P_1^\circ + \gamma_{01}V_{01}$	k_{01}
Initiation	$P_2H \rightarrow P_2^\circ + \gamma_{02}V_{02}$	k_{02}
Initiation	$P_1OOH + \gamma P_1H + (1-\gamma)P_2H \rightarrow 2(1-\gamma_{K1}).\gamma P_1^\circ + 2(1-\gamma_{K1}).(1-\gamma)P_2^\circ \ H_2O + \gamma_1V_1$	k_{11}
Initiation	$P_2OOH + \gamma P_1H + (1-\gamma)P_2H \rightarrow 2(1-\gamma_{K2}).\gamma P_1^\circ + 2(1-\gamma_{K2}).(1-\gamma)P_2^\circ \ H_2O + \gamma_2V_2$	k_{12}
Propagation	$P_1^\circ + O_2 \rightarrow P_1OO^\circ$	k_{21}
Propagation	$P_2^\circ + O_2 \rightarrow P_2OO^\circ$	k_{22}
Propagation	$P_1OO^\circ + P_1H \rightarrow P_1OOH + P_1^\circ$	k_{311}
Propagation	$P_1OO^\circ + P_2H \rightarrow P_1OOH + P_2^\circ$	k_{312}
Propagation	$P_2OO^\circ + P_1H \rightarrow P_2OOH + P_1^\circ$	k_{321}
Propagation	$P_2OO^\circ + P_2H \rightarrow P_2OOH + P_2^\circ$	k_{322}
Termination	$P_1^\circ + P_1^\circ \rightarrow$ inactive products	k_{411}
Termination	$P_1^\circ + P_2^\circ \rightarrow$ inactive products	k_{412}
Termination	$P_2^\circ + P_2^\circ \rightarrow$ inactive products	k_{422}
Termination	$P_1^\circ + P_1OO^\circ \rightarrow$ inactive products	k_{511}
Termination	$P_1^\circ + P_2OO^\circ \rightarrow$ inactive products	k_{512}
Termination	$P_2^\circ + P_1OO^\circ \rightarrow$ inactive products	k_{521}
Termination	$P_2^\circ + P_2OO^\circ \rightarrow$ inactive products	k_{522}
Termination	$P_1OO^\circ + P_1OO^\circ \rightarrow$ inactive products + O_2	k_{611}
Termination	$P_1OO^\circ + P_2OO^\circ \rightarrow$ inactive products + O_2	k_{612}
Termination	$P_2OO^\circ + P_2OO^\circ \rightarrow$ inactive products + O_2	k_{622}

Meaning of symbols are detailed in Table 2.

Symbol	Meaning
P_1H, P_2H	Unreacted susbtrate
$P_1°$, $P_2°$	Alkyl radical
$P_1OO°$, $P_2OO°$	Peroxy radical
P_1OOH, P_2OOH	Hydroperoxide
V_{01}, V_{02}	Volatiles genenerated by thermolysis
σ_{01}, σ_{02}	Yield for volatile generation from substrate decomposition
V_1, V_2	Volatiles generated by thermal oxidation
σ_1, g_2	Yield for volatile generation from oxidation
$\upsilon_{01}M_{v01}$, $\upsilon_{02}M_{v02}$	Contribution to mass loss from substrate decomposition
$\upsilon_{01}M_{v01}$, $\upsilon_{02}M_{v02}$	Contribution to mass loss from oxidation
γ	Probability of P_1H or P_2H attack by any $HO°$ or $P_iO°$ radical
γ_{K1}, γ_{K2}	Yield for cage reaction $P_iO° + HO° \rightarrow$ inactive product (carbonyl)
k_i, k_{ij}	Rate constant
E_i, E_{ij}	Activation energy

Table 2. Signification of kinetic parameters.

The balance equation for initiation are justified in Supplementary Information SI-3. This scheme leads to the differential system given in Supplementary Information SI-4. It allows mass loss to be predicted from :

$$\frac{d\frac{m}{m_0}}{dt}=\frac{32}{\rho}\left(k_{21}\left[P_1°\right]\left[O_2\right]+k_{22}\left[P_2°\right]\left[O_2\right]-k_{611}\left[P_1OO°\right]^2-k_{612}\left[P_1OO°\right]\left[P_2OO°\right]-k_{622}\left[P_2OO°\right]^2\right)-\frac{\left(18+v_1M_{v1}\right.}{\rho}$$

System was solved using ODE23s from Matlab® using the following initial conditions at t = 0, $[P_1°]_0$ = $[P_2°]_0 = [P_1OO°]_0 = [P_2OO°]_0$

The initial substrate concentration was calculated as follows:

① For pure BMI, each monomer holds a diaryl methylene group so that:

345 $$\left[P_1H\right]_0=\frac{\rho}{M_1}=3.6\,mol\,l^{-1}$$

346 M_1 being the molar mass of BMI (358 g mol^{-1})

347 ② For BMI-DABPA 2-1, concentration in BMI comonomer and diallylbisphenol A is weighted by the
348 weight ratio of BMI in the mixture considering that each diallylbisphenol A holds 4 reactive sites:

349 $$\left[P_1H\right]_0=\frac{\rho}{M_1}\cdot\frac{2M_1}{2M_1+M_2}=2.5\,mol\,l^{-1}$$

350 $$\left[P_2H\right]_0=4\frac{\rho}{M_2}\cdot\frac{M_2}{2M_1+M_2}=5\,mol\,l^{-1}$$

351 M_2 being the molar mass of DABPA (308 g mol^{-1})

352 The total initial concentration in hydroperoxide was arbitrarily fixed equal to 0.001 mol l^{-1} so that:

353 - For pure BMI:

354 $$\left[P_1OOH\right]_0=0.001\,mol\,l^{-1}$$

355 - For BMI-DABPA 2-1 copolymer:

356 $$\left[P_1OOH\right]_0=0.00035\,mol\,l^{-1}$$

357 $$\left[P_2OOH\right]_0=0.00065\,mol\,l^{-1}$$

358

359 The oxygen concentration was fixed equal to 0.04 mol l^{-1} consistently with [25].

360

361 The main complexity is the high number of parameters in the kinetic model. Many of them were fixed
362 in order to have the less possible number of adjustable parameters. Here, we implemented the
363 following approach:

364 - Rate constants were first determined for pure BMI and then for BMI-DABPA 2-1.

365 - Under nitrogen, only k_{0i} and k_{4ij} are needed to fit the curves of mass loss. Those values were then
366 utilized for simulating degradation under oxyen without change.

- The rate constants k_{01}, k_{02} and the yields for volatile release were adjusted from the parametric study presented in Figure 2 by fitting the curves under inert atmosphere. Figure 8a illustrates a parametric study for the k_0 value.

- According to the analysis of oxidation mechanisms presented in the previous section, reactive sites were identified because of their bond dissociation energies. It allows the estimation of the rate constants values for the POO° + PH → POOH + P° values from the semi-empirical values proposed by Korcek et al [26]:

$$\log_{10} k_3^{sec-POO^\circ}(30\,^\circ C) = 16.4 - 0.2 * BDE$$

$$E_3^{sec-POO^\circ} = 0.55 \times (BDE - 62.5)$$

$$\log_{10} k_3^{tert-POO^\circ}(30\,^\circ C) = 15.4 - 0.2 * BDE$$

$$E_3^{tert-POO^\circ} = 0.55 \times (BDE - 65)$$

- The rate constants for termination (k_{4ij}, k_{5ij}, k_{6ij}) should in principle be determined from a study under varying oxygen pressures [27]. In the absence of this latter, we used the following assumptions: (i) 10^{10} > k_{4ij} > k_{5ij} >> k_{6ij}, (ii) $k_{5ij} = 5 \times 10^8$ l mol^{-1} s^{-1} and $k_{6ij} = 10^5$ l mol^{-1} s^{-1} keeping in mind that the rate constant for the termination between two POO° (k_{6ij}) mainly influences the kinetics under high oxygen pressures, (iii) $k_{412} = (k_{411} \times k_{422})^{1/2}$ [23,24]. The effect of k_{4ij} is illustrated by the parametric study given in Figure 8f. Let us precise that the termination product of two radicals can be a double bond, consistently with experimental observations (Figure 5).

Finally, k_{1ij}, k_{2ij}, k_{0i} and k_{4ij}, $\square_{Ki}$ were the remaining adjustable parameters. We assumed that $k_{21} = k_{22}$. The results of a parametric study for those constants are depicted in Figures 8b, 8c and 8d. For summarizing:

- k_{1i} was adjusted basing on the initial concavity of the curve in Figure 2. We also checked its consistency with comparable results obtained by Colin et al [17] (Figure 10b).

- k_{2i} was adjusted on the mass loss rate at early stages. It must however be recognized that several k_2, k_4 sets would lead to comparable simulations.

- k_{3ij} were fixed but their influence is depicted for example in Figure 8e.

Another attempt to validate the model was to fit the data by Colin et al [17], despite the fact that the formulation used in their work may not exactly match with the BMI and BMI DABPA 2-1 studied in this

work. Results are given in Figure 9 where two cases were considered: the fictive case of a pure BMI resin and the case of BMI DABPA 2-1 (on which rate constants were adjusted in a consistent manner with rate constants determined from Figure 9).

Finally, it can be seen that kinetic model describes the mass loss kinetics (Figures 2 and 9) in a wide range of temperatures (180 to 375°C) with elementary rate constants obeying Arrhenius law with reasonable activation energies (Figure 10): E_{1i} ~ 140 kJ mol^{-1}, E_{2i} ~ E_{4i} ~ 15 kJ mol^{-1}.

Further improvements can be envisaged in order to optimize the fits under oxidative conditions:

- here, we assumed quasi ideal structures which may not the case for real networks. For example, BMI-DABPA networks can possibly BMI or DABPA homopolymerized sequence. Their reactivity must be understood and some reactions should be added to the model. However, it is first needed to evidence the presence of such sequences in networks.

- the participation of sites having a lower reactivity (such as the –CH-CH-CH-CH- sequence in pure BMI).

- the actual effect of curing degree could also be taken into account [28].

- we assumed that some parameters (namely $\upsilon_1 M_{v1}$, $\upsilon_2 M_{v2}$, $\upsilon_{01} M_{v01}$, $\upsilon_{02} M_{v02}$) remain constant during the whole timescale under consideration which is clearly an approximation.

- in particular, the possibility of retro Diels Alder occurring under nitrogen for BMI-DABPA is to investigate.

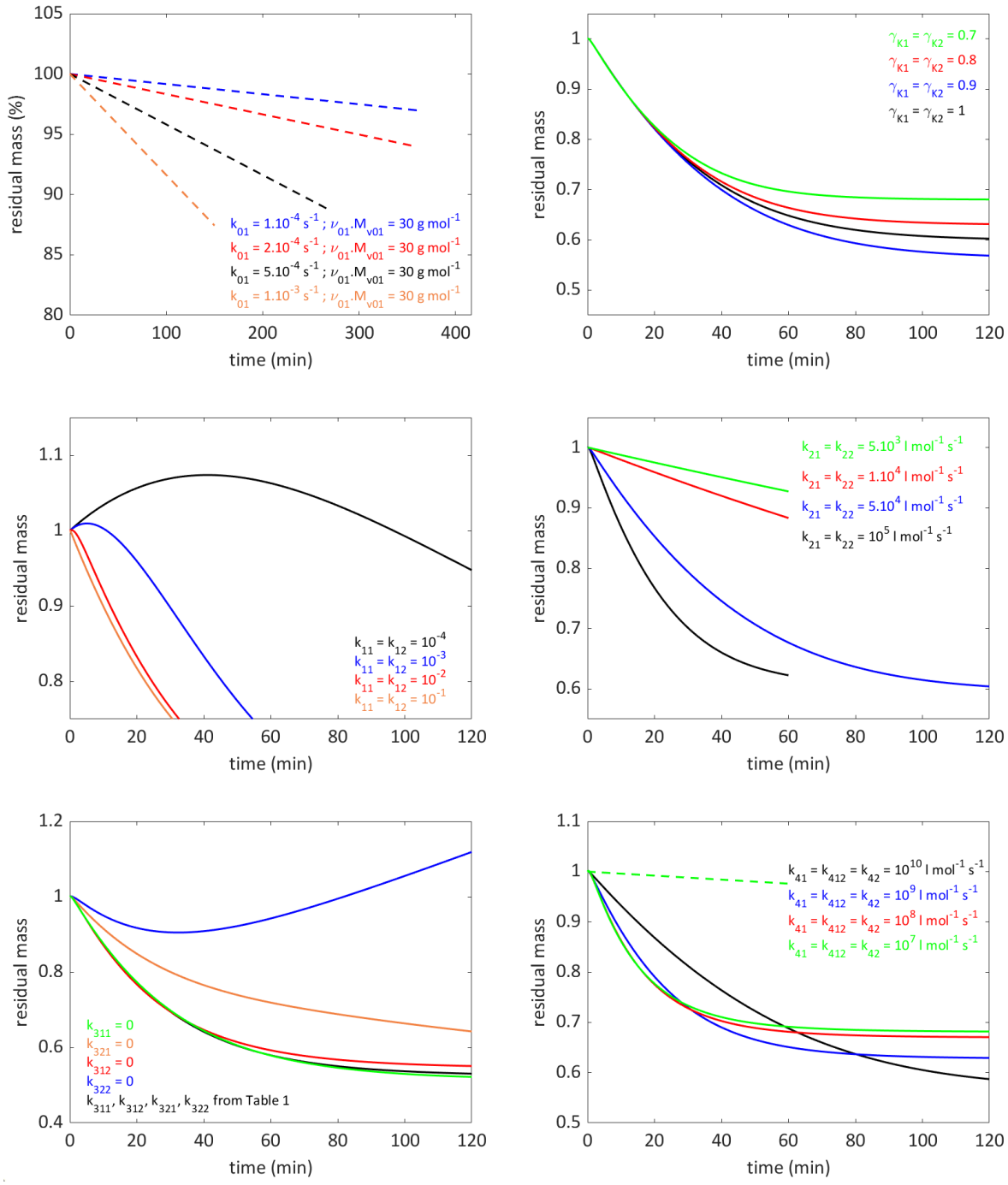

Figure 8. Parametric study with dashed lines: under inert atmosphere, full lines: under oxygen, using with parameters corresponding to 350°C (see Table 2).

	180°C	210°C	240°C	350°C	375°C	E_a (kJ mol^{-1})
k_{11} (s^{-1})	4×10^{-7}	2.75×10^{-6}	2.5×10^{-5}	1.1×10^{-2}	2.75×10^{-2}	142.4
k_{12} (s^{-1})	2.7×10^{-6}	1.65×10^{-5}	1.3×10^{-5}	5.0×10^{-2}	1.4×10^{-1}	139.3
k_{21} (l mol^{-1} s^{-1})	2.5×10^{4}	3.1×10^{4}	3.75×10^{4}	6.5×10^{4}	7.5×10^{4}	13.6
k_{22} (l mol^{-1} s^{-1})	2.5×10^{4}	3.1×10^{4}	3.75×10^{4}	6.5×10^{4}	7.5×10^{4}	13.6
k_{311} (l mol^{-1} s^{-1})	366	768	1912	9450	13200	44.9
k_{321} (l mol^{-1} s^{-1})	17	46	58	292	391	39.1
k_{312} (l mol^{-1} s^{-1})	588	1100	1475	9201	12210	38.0
k_{322} (l mol^{-1} s^{-1})	28	33	75	285	362	32.2
k_{411} (l mol^{-1} s^{-1})	5×10^{8}	7×10^{8}	9×10^{8}	2.2×10^{9}	2.4×10^{9}	20.0
k_{422} (l mol^{-1} s^{-1})	8×10^{8}	1.15×10^{9}	1.5×10^{9}	3.2×10^{9}	3.2×10^{9}	18.4
k_{412} (l mol^{-1} s^{-1})	$(k_{411}\times k_{422})^{0.5}$					0
k_{511} (l mol^{-1} s^{-1})	5×10^{8}	5×10^{8}	5×10^{8}	5×10^{8}	5×10^{8}	0
k_{512} (l mol^{-1} s^{-1})	5×10^{8}	5×10^{8}	5×10^{8}	5×10^{8}	5×10^{8}	0
$k_{512} = k_{521}$ (l mol^{-1} s^{-1})	$(k_{511}\times k_{522})^{0.5}$					0
k_{611}, k_{612}, k_{622}	10^{8}	10^{8}	10^{8}	10^{8}	10^{8}	0
γ_{K1}	1	1	1	1	1	
γ_1	0	0	0	0	0	
γ_{K2}	1	1	1	0.8	0.8	
γ_2	0	0	0	0	0	
$\upsilon_1 M_{v1}$ (g mol^{-1})	25	29	32.5	85	117.5	

$\upsilon_2 M_{v2}$ (g mol^{-1})	45	50	51.5	130	95	
ρ	1300	1300	1300	1300	1300	
k_{01} (s^{-1})	6×10^{-9}	4×10^{-8}	2×10^{-7}	5.5×10^{-5}	1.5×10^{-4}	126.9
$\upsilon_{01} M_{v01}$ (g mol^{-1})	0	0	0	1	4	
k_{02} (s^{-1})	7×10^{-8}	5×10^{-7}	3.0×10^{-6}	8.5×10^{-4}	1.6×10^{-3}	129.8
$\upsilon_{02} M_{v02}$ (g mol^{-1})	0	0	0	1.75	2	

Table 3. Kinetic parameters for simulations given in Figures 2 and 9.

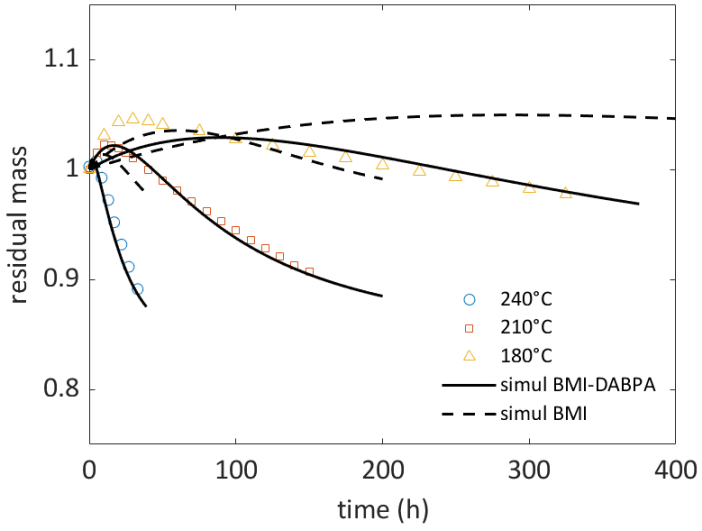

Figure 9. Simulation of results by Colin et al [17] with kinetic model working with $[P_1H]_0$ = 2.5 and $[P_2H]_0$ = 5 mol l^{-1} (BMI-DABMA 2-1) or $[P_1H]_0$ = 3.6 mol l^{-1} and $[P_2H]_0$ = 0 (pure BMI).

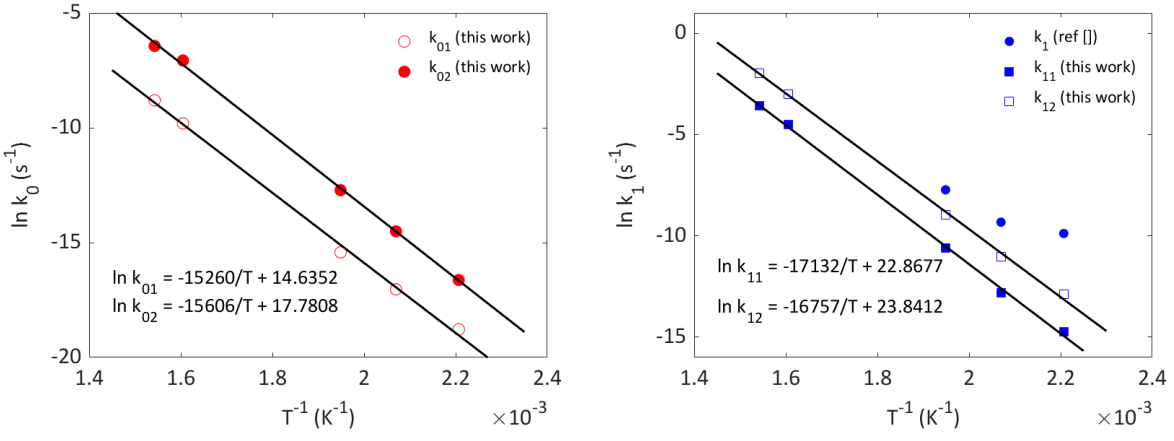

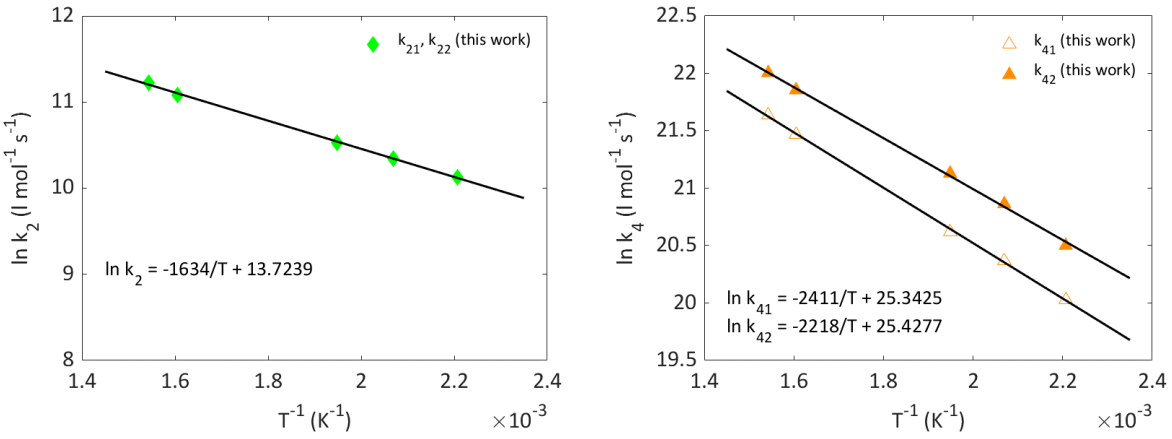

Figure 10. Arrhenius diagram for rate constants.

CONCLUSIONS

In this paper, networks made from bismaleimide and diallylbisphenol A were synthesized and submitted to isothermal ageing at various temperatures under inert atmosphere and or under air. Results clearly show that diallyl comonomer lowers thermal stability of BMI resins. This was confirmed by an estimation of the Bond Dissociation Energies of structural units of BMI and BMI-DABPA since DABPA displays some weak bonds that can more easily undergo homolysis and radical attack. Basing on those observations, a kinetic model for co-oxidation was proposed. The complexity of such modelling tools is the high number of parameters that can influence the simulations. In order to decrease the number of adjustable parameters, some rate constants values were and some other were identified from a parametric study. Finally, the kinetic model displays an encouraging capability to simulate mass loss induced by thermal ageing of BMI based networks as confirmed by comparing its prediction with literature data. Its validation process can be pursued by performing long term ageing runs at lower temperatures.

REFERENCES

[1] M.-F. Grenier-Loustalot, L. Da Cunha. Study of molten-state polymerization of bismaleimide monomers by solid-state13C n.m.r. and FTi.r. Polymer 39 (1998) 1833-1843.

[2] J. Zhu. Curing behavior and properties of 4,4' bismaelimidodiphenylmethane and O,O' Diallyl bisphenol A: effect of peroxides and hybrid silesquioxane addition. Michigan State University (2012).

[3] A. Seris, M. Feve, F. Mechin, J.P. Pascault. Thermally and Anionically Initiated Cure of Bismaleimide Monomers. Journal of Applied Polymer Science 48 (1993) 257-269.

[4] R.J. Iredale, C. Ward, I. Hamerton. Modern advances in bismaleimide resin technology: A 21st century perspective on the chemistry of addition polyimides. Progress in Polymer Science 69 (2017) 1-21.

[5] J. Hao, L. Jiang, X. Cai. Investigation on bismaleimide bearing polysiloxane (BPS) toughening of 4,4′-bismaleimido diphenylmethane (BMI) matrix—synthesis, characterization and toughness. Polymer 37 (1996) 3721-3727.

[6] J. Xu, H. Wu, O.P. Mills, P.A. Heiden. Morphological Investigation of Thermosets Toughened with Novel Thermoplastics. I. Bismaleimide Modified with Hyperbranched Polyester. Journal of Applied Polymer Science 72 (1999) 1065-1076.

[7] Q. Lin, R. Zheng, P. Tian. Preparation and characterization of BMI resin/graphite oxide nanocomposites. Polymer Testing 29 (2010) 537–543

[8] X. Jiang, F. Chu, X. Luo, Y. Hu, W. Hu. Exploring the effects of cardanol-based co-curing agents with different phosphorus structures on the mechanical and flame-retardant properties of bismaleimide resin. Composites Part B: Engineering 241 (2022) 110047.

[9] H. Tang, N. Song, Z. Gao, X. Chen, Q. Zhou. Preparation and properties of high performance bismaleimide resins based on 1,3,4-oxadiazole-containing monomers. European Polymer Journal 43 (2007) 1313-1321.

[10] R. Torrecillas, N. Regnier, B. Mortaigne. Thermal degradation of bismaleimide and bisnadimide networks—products of thermal degradation and type of crosslinking points. Polymer Degradation and Stability 51 (1996) 307-318.

[11] K.S. Santhosh Kumar, C.P. Reghunadhan Nair, R. Sadhana, K.N. Ninan. Benzoxazine–bismaleimide blends: Curing and thermal properties. European Polymer Journal 43 (2007) 5084-5096.

[12] C. Gouri, C.P Reghunadhan Nair, R. Ramaswamy, K.N Ninan. Thermal decomposition characteristics of Alder-ene adduct of diallyl bisphenol A novolac with bismaleimide: effect of stoichiometry, novolac molar mass and bismaleimide structure. European Polymer Journal 38 (2002) 503-510.

[13] M. Neda, K. Okinaga, M. Shibata. High-performance bio-based thermosetting resins based on bismaleimide and allyl-etherified eugenol derivatives. Materials Chemistry and Physics 148 (2014) 319-327.

[14] X. Colin, C. Marais, J. Verdu. Kinetic modelling and simulation of gravimetric curves: application to the oxidation of bismaleimide and epoxy resins. Polymer Degradation and Stability 78 (2002) 545-553.

[15] X. Colin, C. Marais, J. Verdu. Thermal oxidation kinetics for a poly(bismaleimide). Journal of Applied Polymer Science Volume 82 (2001) 3418-3430.

[16] C. Daily, D.J. Barnard, R.W. Jones, J.F. McClelland, N. Bowler. Dielectric and infrared inference of thermo-oxidative aging of a bismaleimide composite material. Composites Part B: Engineering 101 (2016) 167-175.

[17] X. Colin, C. Marais, J. Verdu. Kinetic modelling and simulation of gravimetric curves: application to the oxidation of bismaleimide and epoxy resins. Polymer Degradation and Stability 78 (2002) 545-553.

[18] J. Decelle, N. Huet, V. Bellenger. Oxidation induced shrinkage for thermally aged epoxy networks. Polymer Degradation and Stability 81 (2003) 239-248.

[19] S. Konica, T. Sain. A homogenized large deformation constitutive model for high temperature oxidation in fiber-reinforced polymer composites. Mechanics of Materials 160 (2021) 103994.

[20] L. Xue, W. Fan, F. Wu, Y. Zhang, K. Guo, J. Li, L. Yuan, W. Dang, R. Sun. The influence of thermo-oxidative aging on the electromagnetic absorbing properties of 3D quasi-isotropic braided carbon/glass bismaleimide composite. Polymer Degradation and Stability 168 (2019) 108941.

[21] W. Shaoquan, D. Shangli, G. Yu, S. Yungang. Thermal ageing effects on mechanical properties and barely visible impact damage behavior of a carbon fiber reinforced bismaleimide composite. Materials & Design 1155 (2017) 213-223.

[22] R. Delannoy, V. Tognetti, E. Richaud. Experimental and theoretical insights on the thermal oxidation of epoxy-amine networks. Polymer Degradation and Stability 206 (2022) 110188.

[23] E. Richaud, B. Fayolle, J. Verdu, J. Rychlý. Co-oxidation kinetic model for the thermal oxidation of polyethylene-unsaturated substrate systems. Polymer Degradation and Stability 98 (2013) 1081-1088.

[24] M. Touffet, P. Smith, O. Vitrac. A comprehensive two-scale model for predicting the oxidizability of fatty acid methyl ester mixtures. Food Research International 173 (2023) 113289.

[25] X. Colin, C. Marais, J. Verdu. Thermal oxidation kinetics for a poly(bismaleimide). Journal of Applied Polymer Science 82 (2001) 3418-3430.

[26] S. Korcek, J.H.B. Chenier, J.A. Howard, K.U. Ingold. Absolute Rate Constants for Hydrocarbon Autoxidation. XXI. Activation Energies for Propagation and the Correlation of Propagation Rate Constants with Carbon–Hydrogen Bond Strengths. Canadian Journal of Chemistry 50 (1972) 2285 – 2297.

[27] E. Richaud, F. Farcas, P. Bartoloméo, B. Fayolle, L. Audouin, J. Verdu. Effect of oxygen pressure on the oxidation kinetics of unstabilised polypropylene. Polymer Degradation and Stability 91 (2006) 398-405.

[28] J. Delozanne, J.S. Montana, A. Guinault, N. Desgardin, N. Cuvillier, E. Richaud. Thermal ageing of bonded assemblies. Effect of adhesive curing degree. The Journal of Adhesion 99 (2023), 911-929.